

Wearable and humidity-resistant biomaterials-based triboelectric nanogenerator for high entropy energy harvesting and self-powered sensing

Ning Zheng^{1,2,§}, Jiehui Xue^{1,3,§}, Yang Jie^{1,2,§}, Xia Cao^{1,2,4} (✉), and Zhong Lin Wang^{1,2,5} (✉)

¹ CAS Center for Excellence in Nanoscience, Beijing Institute of Nanoenergy and Nanosystems, Chinese Academy of Sciences, Beijing 100083, China

² School of Nanoscience and Technology, University of Chinese Academy of Sciences, Beijing 100049, China

³ School of Resources Environment and Materials, Guangxi University, Nanning 530004, China

⁴ Research Center for Bioengineering and Sensing Technology, Beijing Key Laboratory for Bioengineering and Sensing technology, School of Chemistry and Biological engineering, and Beijing Municipal Key Laboratory of New Energy Materials and Technologies, University of Science and Technology Beijing, Beijing 100083, China

⁵ School of Materials Science and Engineering, Georgia Institute of Technology, Atlanta, Georgia 30332, USA

[§] Ning Zheng, Jiehui Xue, and Yang Jie contributed equally to this work.

© Tsinghua University Press 2022

Received: 13 January 2022 / Revised: 26 February 2022 / Accepted: 11 March 2022

ABSTRACT

Triboelectric nanogenerator (TENG) provides a new solution to the energy supply by harvesting high entropy energy. However, wearable electronic devices have high requirements for flexible, humidity-resistant, and low-cost TENG. Here, environment-friendly and multi-functional wheat starch TENG (S-TENG) was made by a simple and green method. The open-circuit voltage and short-circuit current of S-TENG are 151.4 V and 47.1 μA , respectively. S-TENG can be used not only to drive and intelligently control electronic equipment, but also to effectively harvest energy from body movements and wind. In addition, the output of S-TENG was not negatively affected with the increase in environmental humidity, but increased abnormally. In the range of 20% RH–80% RH, S-TENG can be potentially used as a sensitive self-powered humidity sensor. The S-TENG paves the way for large-scale preparation of multi-functional biomaterials-based TENG, and practical application of self-powered sensing and wearable devices.

KEYWORDS

triboelectric nanogenerator, natural polymers, humidity-resistant, wearable smart device, self-powered sensing

1 Introduction

Nowadays, the global energy supply system is facing unprecedented challenges, due to the climate warming and the depletion of fossil fuels. Some clean and renewable energy sources have been used as the sustainable response, such as sun, wind, and water. However, harvesting these forms of energy is often costly and the equipment is bulky and complex. In 2012, the Wang's group first invented triboelectric nanogenerator (TENG) with low cost, small volume, and simple structure [1]. So far, TENG has been developed to harvest almost any irregular and distributed mechanical energy (high entropy energy [2]) in the environment, such as mechanical energy [3–6], wind energy [7–12], ocean energy [13–18], raindrop energy [19–23], etc. TENG can be also widely used as self-powered sensor [24–29], utilizing its electrical output signal to actively detect dynamic processes caused by mechanical disturbances. So, flexible TENGs are very suitable for power supply and sensing design of wearable devices.

Most of TENGs are currently made based on the synthetic polymers. However, these substances are difficult to degrade in the natural environment. In contrast, natural polymers not only are low-cost and abundant, but also have excellent biodegradability,

good film-forming property, and good large-scale processing characteristic. The application of these natural polymers is of great significance to the sustainable development of TENG. In fact, TENG based on natural materials has received more and more attention [30–37]. However, the processing methods of natural materials are often complex, and the performances of TENGs are unstable after being used for a long time especially in humid conditions.

In this work, a simple and green method was proposed to prepare wheat starch based TENG (S-TENG). The open-circuit voltage (V_{oc}), short-circuit current (I_{sc}), and power density of S-TENG (25 cm^2 , frequency of 4 Hz) are 151.4 V, 47.1 μA , and 113.2 $\mu\text{W}\cdot\text{cm}^{-2}$, respectively. S-TENG can light up 100 light-emitting diodes (LEDs) simultaneously. As a stable and reliable power source, S-TENG can power electronic watches and hygrometers by charging commercial capacitors. As a wearable energy harvester, S-TENG was attached to different parts of human body to harvest energy and monitor the human movement, including walking, running, bowing, and raising the head. In addition, S-TENG was installed on a scarecrow to harvest energy from slapping and wind. By pressing the single electrode S-

Address correspondence to Xia Cao, caoxia@binn.cas.cn; Zhong Lin Wang, zlwang@gatech.edu

TENG (SS-TENG) with a finger, intelligent control of timers was realized. Furthermore, S-TENG can be used as a potential humidity sensor. It is worth noting that the output of S-TENG enhances with the increase of humidity, which makes up for the shortcomings of ordinary TENGs. We believe that this work will pave the way for the construction of low-cost, environmentally friendly, and multi-functional bio-based TENG, which is a vital component for self-powered sensing and wearable devices.

2 Experimental

2.1 Preparation of wheat starch film

Wheat starch (4.0 g), glycerin (1 mL), and sodium carboxymethyl cellulose (CMC, 0.25 g) were added into the 75 mL of deionized water and kept stirring at 75 °C for half an hour. After that, the dissolved starch solution was poured into an acrylic mold. Then the whole mold was put into the oven and dried at 60 °C for 3 h to form a film.

2.2 Preparation of S-TENG

Starch film and fluorinated ethylene propylene (FEP) were cut to the required size and used as the triboelectric layers. Aluminum (Al) foils were pasted on both of the triboelectric layers to serve as the conductive electrodes, and wires were passed on aluminum foils for easy connection to the external circuit.

2.3 S-TENG for harvesting biomechanical energies and monitoring human motion

A soft and skin-friendly cloth was used as the base. Wheat starch film and FEP were used as the triboelectric layers, and aluminum foils were used as the conductive electrodes. 1.5 mm thick 3 M tape was used as spacers to create a certain gap between the starch film and FEP.

2.4 Test and characterization

The tensile properties of the wheat starch film were tested by peel strength tester (YI-s71). S-TENG based on acrylic substrate was installed on a linear motor to simulate the contact-separation process. The open-circuit voltage, short-circuit current, and transferred charge of S-TENG were measured by a Keithley 6514 system electrometer with computer measurement software written in LabVIEW.

2.5 The electrical performance test of S-TENG under different humidity

The S-TENG, humidifier, and hygrometer were put into a closed acrylic box. The humidifier was used to simulate 20%–80% seven different environmental relative humidity conditions, and the hygrometer was used to measure the relative humidity in the box. Then the output voltage and current of S-TENG under different environmental relative humidity were measured by electrometer.

3 Results and discussion

Wheat is a cereal crop that is widely grown all over the world. As a processed product of wheat, wheat starch is a natural polymer material with abundant sources and low cost. Here, a simple and non-polluting method was used to turn wheat starch into wheat starch film for the manufacture and application of TENG. Figure 1(a) shows a photo of wheat starch and wheat starch film (dimension: 6 cm × 7 cm, thicknesses: 0.15 mm). The prepared starch film shows excellent transparency. When the starch film is placed on a paper, the printed text (triboelectric nanogenerators)

on the paper can be clearly observed. As shown in Figs. 1(b)–1(d), the starch film is light in weight and has certain flexible and tensile properties. According to the mass and volume of starch film, the density of the film is about 1.519 g·cm⁻³. The breaking extension and breaking strength of wheat starch film are 24.97% and 4.26 MPa, respectively. Therefore, the starch film has great application prospects in transparent or flexible electronic devices. Figure 1(e) shows the fabrication of S-TENG based on a starch film, which works in a typical vertical contact-separation mode. Starch film and FEP were used as the triboelectric layers, and aluminum foils were pasted on both of the triboelectric layers to serve as the electrodes. The V_{oc} , I_{sc} and transfer charge of S-TENG with a dimension of 5 cm × 5 cm under the working frequency of 4 Hz, are 151.4 V, 47.1 μA, and 110 nC, respectively (Figs. 1(f)–1(h)).

The working mechanism of S-TENG based on the vertical contact-separation mode is illustrated in Fig. 2(a). It works by the coupling of triboelectrification and electrostatic induction. In the initial state, no charge is generated, and there is no potential difference between the two aluminum electrodes. When FEP contacts with the starch film under the action of external force, charge transfer occurs on the surface of two materials due to the triboelectric effect. Electrons on the surface of the starch film are transferred to the FEP surface, thus making the FEP surface negatively charged and the starch film positively charged (Fig. 2(a)(I)). After the two triboelectric layers are separated, the potential difference that drives electrons to flow is generated between the two attached electrodes due to electrostatic induction (Fig. 2(a)(II)). When the FEP is completely returned to its original position, it eventually reaches equilibrium (Fig. 2(a)(III)). If the external force is applied again to make the FEP and the starch film contact each other, the potential between two electrodes will gradually disappear. And the electrostatic induced charge will flow back through the external load to compensate for the potential difference, thus generates reverse electric current (Fig. 2(a)(IV)). When the FEP and the starch film are in complete contact, the equilibrium state is reached again (Fig. 2(a)(I)). Another working cycle will restart, and S-TENG will generate alternating currents with periodic contact and separation.

The potential distribution of a working cycle of S-TENG is simulated by COMSOL software. The size of the model is 5 cm × 5 cm, and the charge density on the starch film and FEP is respectively set to 10 and -10 μC·m⁻². Figure 2(b) shows that the electric displacement field of aluminum electrodes varies periodically with the contact-separation of the FEP and the starch film, which will induce the electrons in the circuit to move to obtain periodic signals. This is consistent with the explanation of working mechanism of S-TENG.

The output of S-TENG is closely related to the working frequency, contact area, and contact materials, so S-TENG based on acrylic substrate is installed on a linear motor to test the performance. When the working frequency of the linear motor increases from 0.5 to 4 Hz, the V_{oc} and I_{sc} of S-TENG (5 cm × 5 cm) both increase (Figs. 3(a) and 3(b)). Next, the V_{oc} and I_{sc} of S-TENG with different contact areas are tested under the working frequency of 2 Hz. The results show that the large contact area can improve the output of S-TENG (Figs. 3(c) and 3(d)). Besides, five kinds of materials are selected as the triboelectric layer opposite to the starch film to compare the output of S-TENG. As shown in Fig. 3(e), the electron affinity of FEP and starch film is quite different, which can make the S-TENG more excellent performance.

In addition, environmental humidity will seriously affect the performance of TENG. Therefore, the relative humidity test of S-TENG was carried out in a self-made humidity chamber. Figure

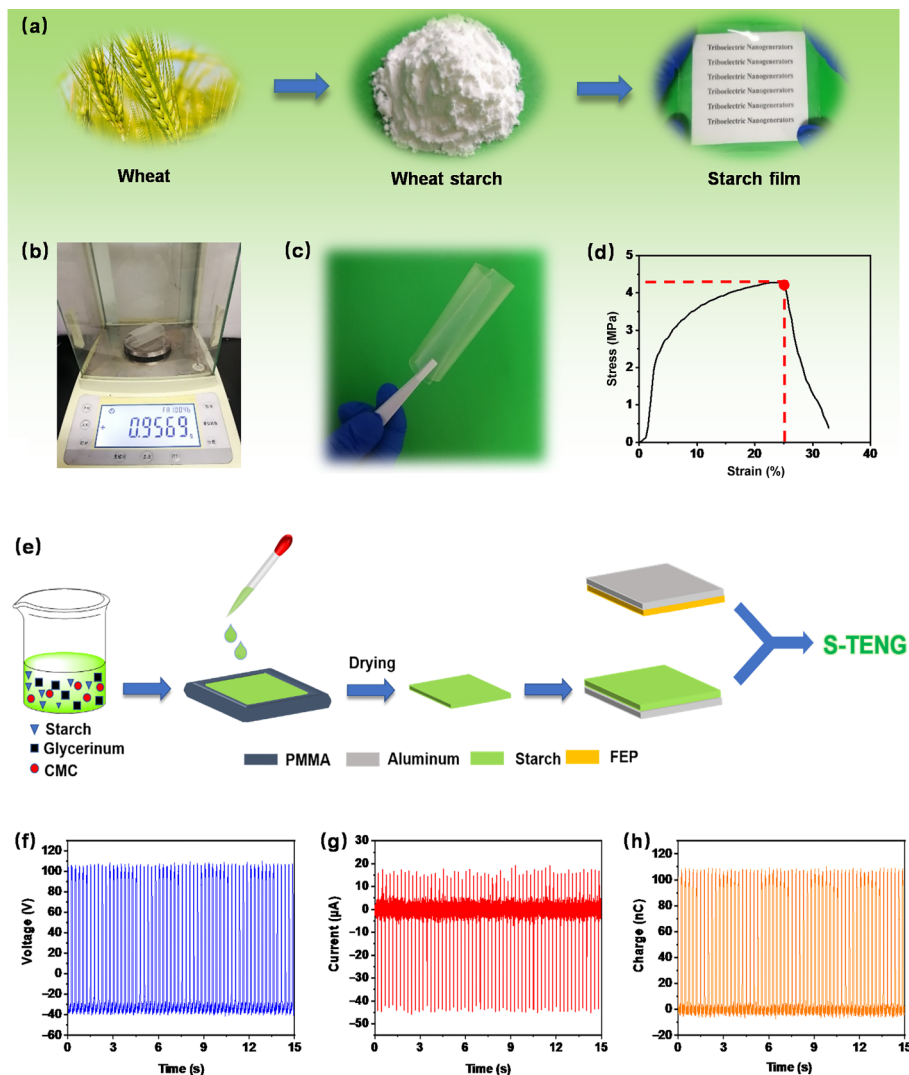


Figure 1 (a) Photographs of wheat, wheat starch, and starch film. (b) Weight and (c) flexibility of the wheat starch film. The wheat starch film has a size of 6 cm \times 7 cm and a thickness of about 0.15 mm. (d) The tensile property curve of wheat starch film. (e) Schematic diagram of the fabricating process of S-TENG. (f) Open-circuit voltage, (g) short-circuit current, and (h) transfer charge of S-TENG (working frequency: 4 Hz, contact area: 5 cm \times 5 cm).

3(f) is the schematic diagram of the device during the humidity test. A linear relationship between the output of S-TENG and relative humidity is observed in the relative humidity range of 20% RH to 80% RH, and the coefficients of determination of fitting curves are 0.998 and 0.987, respectively (Fig. 3(g)). It shows that S-TENG is a potential and promising self-powered humidity sensor to detect environmental humidity. However, it is worth noting that the output of S-TENG increases significantly with the increase of humidity, which is different from most of TENGs [31, 32, 35]. In a high humidity environment, the rich hydroxyl groups of starch molecules will spontaneously form hydrogen bonds with water molecules, thereby fixing the water molecules on the surface of the starch film [38, 39]. As a result, water molecules can work as an electropositive material to make S-TENG obtain a higher output.

To further evaluate the performance of S-TENG, the resistance dependence was investigated by connecting S-TENG with different resistors. As shown in Fig. 3(h), the voltage gradually increases and then tends to be almost unchanged, when the resistance increases from 1,000 Ω to 100 M Ω . But the current shows opposite trend to the voltage due to the ohmic loss. The inset is the circuit diagram of the S-TENG connected with the variable resistor. The power density of S-TENG is shown in Fig. 3(i). When the external resistance is 8 M Ω , the instantaneous power density reaches the maximum value of 113.2 $\mu\text{W}\cdot\text{cm}^{-2}$. S-

TENG can not only be a power source that successfully drives many electronic devices and charges energy storage devices, but also have a wide range of applications in the self-powered sensor.

The durability and stability of S-TENG are also crucial to its practical applications. As shown in Fig. 4(a), S-TENG was subjected to 5,000 times of continuous durability test under the working frequency of 2 Hz. The result shows that the V_{oc} of S-TENG increased slightly, which may be the slight deformation of the starch film surface in the number of cycles of pressing and releasing. However, I_{sc} of S-TENG is basically stable with no obvious changes. In addition, under the same test conditions, the V_{oc} and I_{sc} of S-TENG were tested for 14 consecutive days. It can be found that the S-TENG is relatively stable (Fig. 4(b)). This result reflects the superior stability and durability of S-TENG.

As a power source, S-TENG can be used to drive multiple electronic devices. As shown in Fig. 4(c), S-TENG was placed on a linear motor to make FEP and starch film contact and separate periodically. When the linear motor started working, 100 LEDs forming the shape of wheat were lit brightly (Fig. 4(d) and Video ESM1). This proves that S-TENG has an excellent ability to convert mechanical energy into electrical energy. Besides, the electrical energy generated by S-TENG can be stored in capacitor to drive some electronic devices. Figure 4(e) shows voltage of commercial different capacitors charged by the S-TENG under the working frequency of 2 Hz. Within 120 s, the voltage of 10 μF

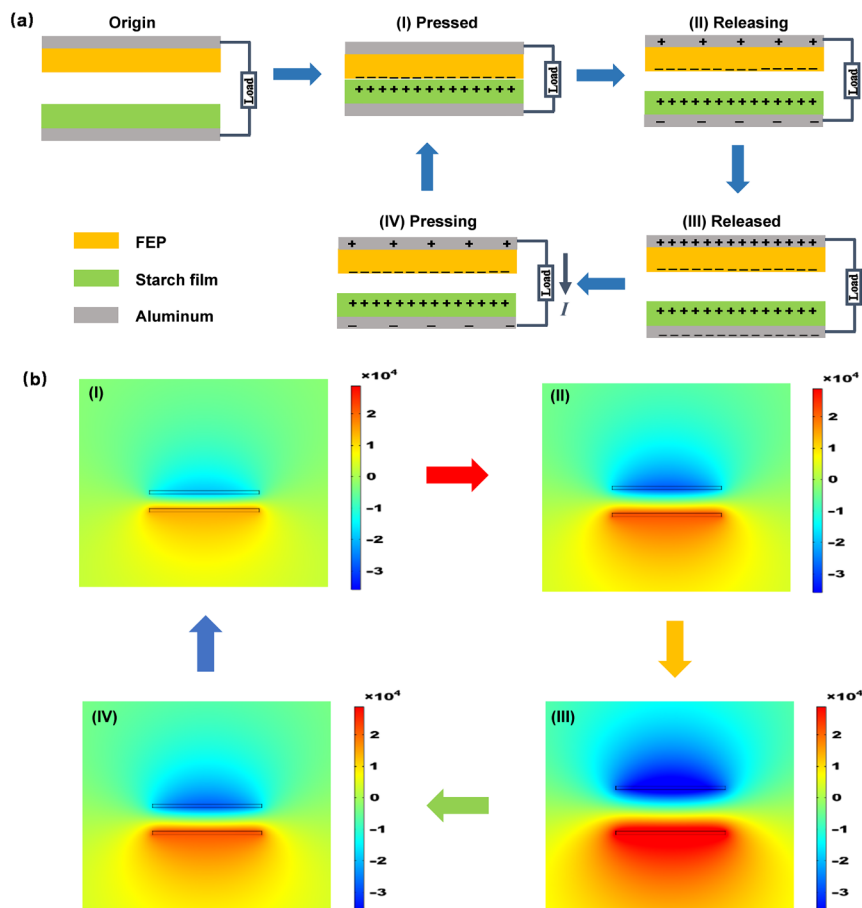


Figure 2 (a) Working mechanism of the S-TENG. (b) The space potential distribution of S-TENG is simulated by COMSOL software.

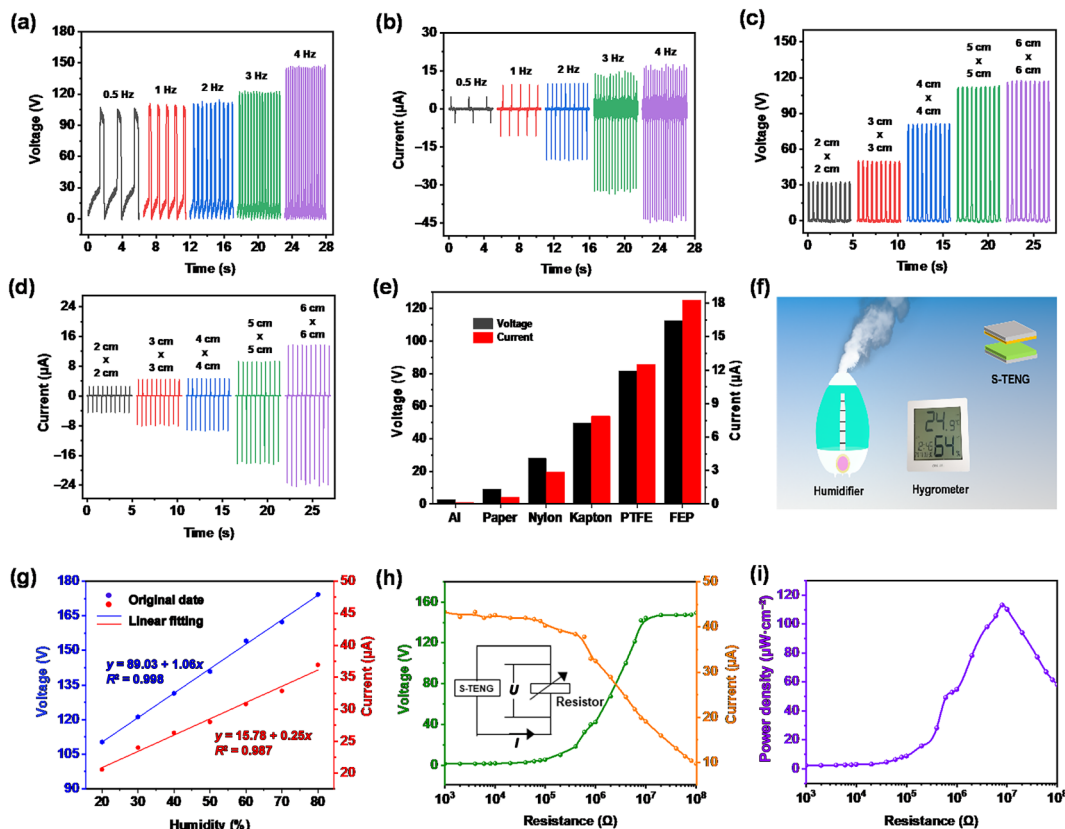


Figure 3 (a) V_{oc} and (b) I_{sc} of S-TENG under different working frequencies. (c) V_{oc} and (d) I_{sc} of S-TENG with different contact areas. (e) Outputs of S-TENG assembled with wheat starch and different triboelectric materials. (f) The schematic diagram of the device during humidity test. (g) The fitting curves of V_{oc} and I_{sc} at relative humidity (20% RH to 80% RH) (working frequency: 2 Hz, contact area: 5 cm x 5 cm). (h) Output voltage, current, and (i) power density under variable load resistance (working frequency: 4 Hz, contact area: 5 cm x 5 cm).

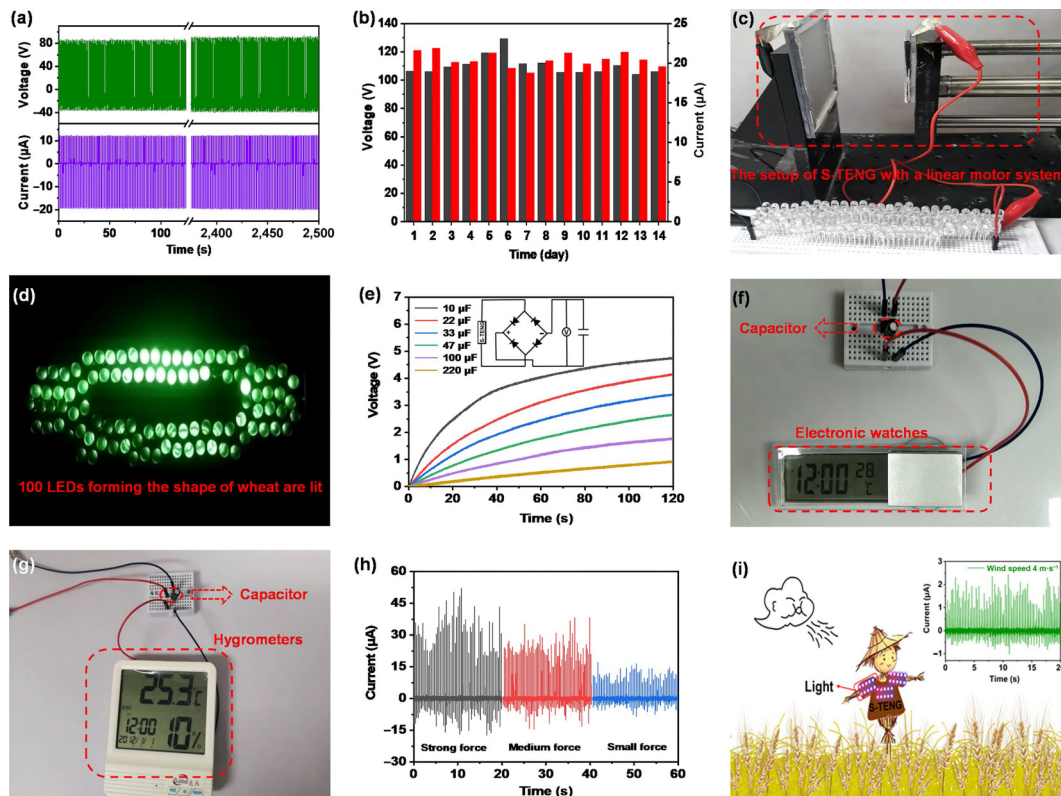


Figure 4 (a) Durability test of S-TENG at 5,000 cycles. (b) Stability test of S-TENG for 14 consecutive days. (c) The setup of S-TENG with a linear motor system and 100 LEDs forming the shape of wheat. (d) Photograph of the 100 LEDs lit up by S-TENG. (e) Voltage profile of different capacitors (10, 22, 33, 47, 100, and 220 μF) charged by the S-TENG. The illustration represents the working circuit of the S-TENG for charging capacitors. (f) An electronic watch and (g) a hygrometer driven by the capacitor charged by the S-TENG (working frequency: 2 Hz, contact area: 5 cm \times 5 cm). (h) The output current under different strength slapping. (i) S-TENG harvest wind to better drive out birds. The illustration shows the current at a wind speed of 4 $\text{m}\cdot\text{s}^{-1}$.

capacitor can reach 4.8 V, the voltage of 47 μF capacitor can reach 2.7 V, and the voltage of 220 μF capacitor can be charged to 1 V. It can be seen that the charging is fast and large-capacity capacitors have better storage capacity but they take longer time to reach the desired voltage. As shown in Figs. 4(f) and 4(g), the capacitors charged by S-TENG can successfully power multiple portable electronic devices, such as electronic watches and hygrometers (Videos ESM2 and ESM3). In addition, two triboelectric layers and electrodes of S-TENG were installed on a scarecrow to harvest energy from slapping and wind. The maximum output current of the slap reaches 49.2 μA (Fig. 4(h)). In the case of a wind speed of 4 $\text{m}\cdot\text{s}^{-1}$, the current reaches 2.5 μA . It can be used to help farmers better guard the fields to prevent birds from destroying crops by powering the warning lights (Fig. 4(i)).

In order to better harvest human energy and monitor human movement, the soft skin-friendly cloth was used as the substrate of S-TENG (Fig. 5(a)). As exhibited in Figs. 5(b)–5(d), the S-TENG can harvest energy from hand, wrist, and arm movements. Moreover, the S-TENG can be used as a human motion sensor. As shown in Fig. 5(e), the S-TENG attached to the neck was used to track the head movements. It can be clearly seen that the generated voltage was higher in the case of head up than head down. Figure 5(f) illustrates self-powered sensing of human walking and running by using S-TENG. When a person wears the S-TENG on the knee, different signals can be recorded at each step. The output voltage increased from ~ 2.3 to ~ 13.8 V, when the person moved from walking to running. Moreover, the timer can be adjusted intelligently by touching and releasing the starch film with the finger (Video ESM4). Figures 5(g) and 5(h) show the circuit of the smart timer controlled by the S-TENG working in a single electrode mode (SS-TENG), which can be integrated into a wearable device. The intelligent control of timer is simply realized by the finger pressing (Fig. 5(i)). Due to the coupling effect of triboelectrification and electrostatic induction, SS-TENG generates

an electrical signal as a trigger signal after the finger and starch film complete a contact-separation process. The trigger signal will be received and processed by the signal receiving module and the processing module in the external circuit. The timer realizes intelligent regulation of start and stop. These results demonstrate that S-TENG is efficient and promising for harvesting energy and monitoring human movements, as well as intelligently controlling.

4 Conclusions

In summary, the wheat starch film for S-TENG was prepared through a simple, non-polluting, and large-scale method. The outputs V_{oc} and I_{sc} of S-TENG are 151.4 V and 47.1 μA respectively, and the measured power density is 113.2 $\mu\text{W}\cdot\text{cm}^{-2}$. The output of S-TENG shows a linear upward trend with the increase of environmental humidity, which demonstrates the application prospect in self-powered humidity sensing. As a power source, S-TENG can successfully light up 100 LEDs, and the mechanical energies harvested by S-TENG can be stored in capacitors to power electronic watch and hygrometer. In addition, S-TENG was installed on a scarecrow to harvest the energy of slapping and wind. More importantly, the S-TENG is capable of harvesting biomechanical energies and monitoring human motion. The self-powered wearable timing device can be also intelligently controlled through simply pressing. This work paves the way for the construction of low-cost, environmentally friendly, and multi-functional biomaterials-based TENG to utilize the high entropy energy. The simplest materials and methods were selected for environmental protection in this work. Output electrical properties of S-TENG can be further improved by modification. In this way, the energy harvesting and application capabilities of S-TENG will be implemented more efficiently.

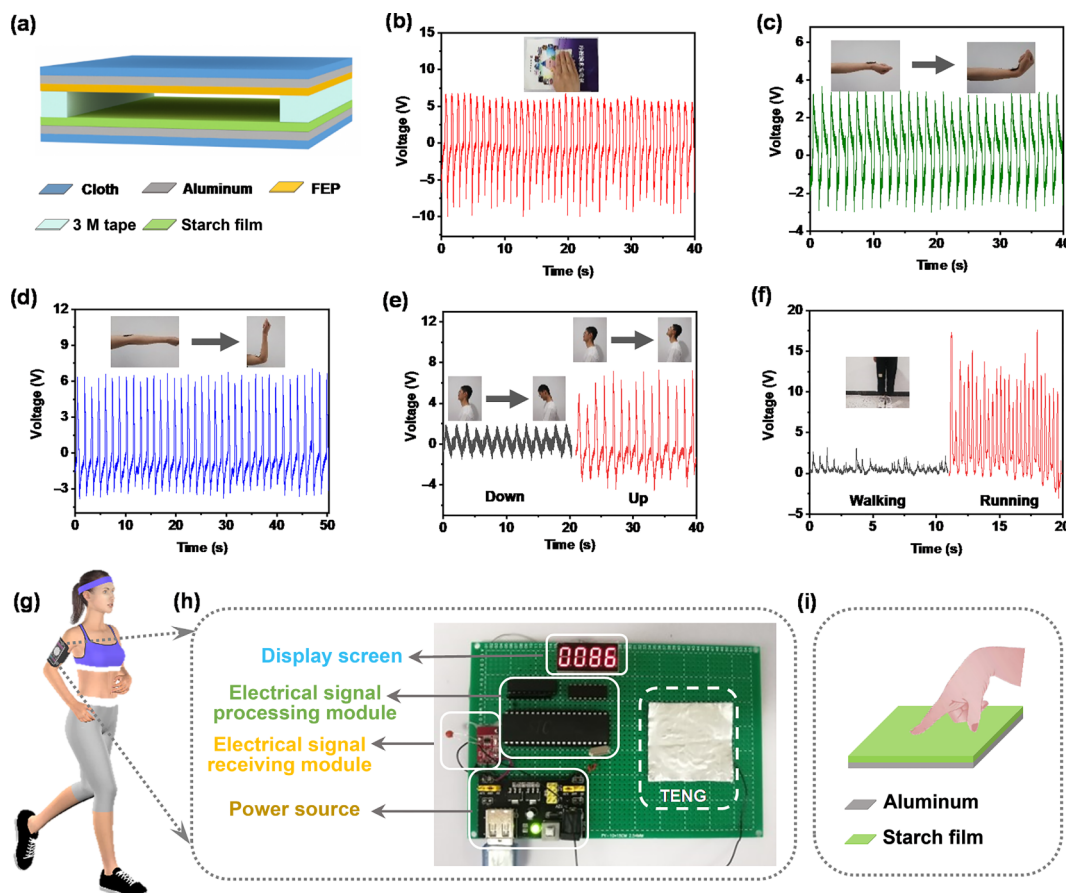


Figure 5 (a) A diagram of the S-TENG with an effective size of 4 cm × 4 cm for human energy harvesting and behavior monitoring. (b)–(d) Voltage responses to human joint motion from the hand, wrist, and arm. (e) and (f) The S-TENG was used as a human motion sensor to detect the movement of the neck and leg of the human body. (g) Schematic diagram of S-TENG based wearable timer used for human body motion timing. (h) Photo of 86 s after the timing triggered by finger pressing on the single electrode S-TENG. (i) The intelligent control of the timer is realized by pressing of the finger.

Acknowledgements

This work was financially supported by the National Key R & D Project from Ministry of Science and Technology, China (Nos. 2016YFA0202702 and 2016YFA0202701) and the Key Research Program of Frontier Sciences, CAS (No. ZDBS-LY-DQC025). Patents have been filed to protect the reported inventions.

Electronic Supplementary Material: Supplementary material (Video ESM1: 100 LEDs were lit by S-TENG mounted on a linear motor. Video ESM2: An electronic watch can be driven by the capacitor charged by the S-TENG. Video ESM3: A hygrometer can be driven by the capacitor charged by the S-TENG. Video ESM4: The timer can be adjusted intelligently by the finger pressing) is available in the online version of this article at <https://doi.org/10.1007/s12274-022-4321-7>.

References

- [1] Fan, F. R.; Tian, Z. Q.; Wang, Z. L. Flexible triboelectric generator. *Nano Energy* **2012**, *1*, 328–334.
- [2] Wang, Z. L. Entropy theory of distributed energy for internet of things. *Nano Energy* **2019**, *58*, 669–672.
- [3] Liu, Y.; Chen, B. D.; Li, W.; Zu, L. L.; Tang, W.; Wang, Z. L. Bioinspired triboelectric soft robot driven by mechanical energy. *Adv. Funct. Mater.* **2021**, *31*, 2104770.
- [4] Liu, C. R.; Zhang, N.; Li, J. Q.; Dong, L. X.; Wang, T.; Wang, Z. K.; Wang, G. F.; Zhou, X. F.; Zhang, J. Harvesting ultralow frequency (< 1 Hz) mechanical energy using triboelectric nanogenerator. *Nano Energy* **2019**, *65*, 104011.
- [5] Xia, K. Q.; Zhu, Z. Y.; Zhang, H. Z.; Du, C. L.; Xu, Z. W.; Wang, R. J. Painting a high-output triboelectric nanogenerator on paper for harvesting energy from human body motion. *Nano Energy* **2018**, *50*, 571–580.
- [6] Lu, X. H.; Xu, Y. H.; Qiao, G. D.; Gao, Q.; Zhang, X. S.; Cheng, T. H.; Wang, Z. L. Triboelectric nanogenerator for entire stroke energy harvesting with bidirectional gear transmission. *Nano Energy* **2020**, *72*, 104726.
- [7] Lin, H. B.; He, M. H.; Jing, Q. S.; Yang, W. F.; Wang, S. T.; Liu, Y.; Zhang, Y. L.; Li, J.; Li, N.; Ma, Y. W. et al. Angle-shaped triboelectric nanogenerator for harvesting environmental wind energy. *Nano Energy* **2019**, *56*, 269–276.
- [8] Wang, Y. Q.; Yu, X.; Yin, M. F.; Wang, J. L.; Gao, Q.; Yu, Y.; Cheng, T. H.; Wang, Z. L. Gravity triboelectric nanogenerator for the steady harvesting of natural wind energy. *Nano Energy* **2021**, *82*, 105740.
- [9] Zhang, C. G.; Liu, Y. B.; Zhang, B. F.; Yang, O.; Yuan, W.; He, L. X.; Wei, X. L.; Wang, J.; Wang, Z. L. Harvesting wind energy by a triboelectric nanogenerator for an intelligent high-speed train system. *ACS Energy Lett.* **2021**, *6*, 1490–1499.
- [10] Zhang, L.; Zhang, B. B.; Chen, J.; Jin, L.; Deng, W. L.; Tang, J. F.; Zhang, H. T.; Pan, H.; Zhu, M. H.; Yang, W. Q. et al. Lawn structured triboelectric nanogenerators for scavenging sweeping wind energy on rooftops. *Adv. Mater.* **2016**, *28*, 1650–1656.
- [11] Wang, Y.; Yang, E.; Chen, T. Y.; Wang, J. Y.; Hu, Z. Y.; Mi, J. C.; Pan, X. X.; Xu, M. Y. A novel humidity resisting and wind direction adapting flag-type triboelectric nanogenerator for wind energy harvesting and speed sensing. *Nano Energy* **2020**, *78*, 105279.
- [12] Ren, Z. W.; Wang, Z. M.; Wang, F.; Li, S. T.; Wang, Z. L. Vibration behavior and excitation mechanism of ultra-stretchable triboelectric nanogenerator for wind energy harvesting. *Extreme Mech. Lett.* **2021**, *45*, 101285.
- [13] Cheng, P.; Liu, Y. N.; Wen, Z.; Shao, H. Y.; Wei, A. M.; Xie, X. K.; Chen, C.; Yang, Y. Q.; Peng, M. F.; Zhuo, Q. Q. et al. Atmospheric pressure difference driven triboelectric nanogenerator for efficiently harvesting ocean wave energy. *Nano Energy* **2018**, *54*, 156–162.

- [14] Xu, M. Y.; Zhao, T. C.; Wang, C.; Zhang, S. L.; Li, Z.; Pan, X. X.; Wang, Z. L. High power density tower-like triboelectric nanogenerator for harvesting arbitrary directional water wave energy. *ACS Nano* **2019**, *13*, 1932–1939.
- [15] Zhang, D. H.; Shi, J. W.; Si, Y. L.; Li, T. Multi-grating triboelectric nanogenerator for harvesting low-frequency ocean wave energy. *Nano Energy* **2019**, *61*, 132–140.
- [16] Liu, G. L.; Xiao, L. F.; Chen, C. Y.; Liu, W. L.; Pu, X. J.; Wu, Z. Y.; Hu, C. G.; Wang, Z. L. Power cables for triboelectric nanogenerator networks for large-scale blue energy harvesting. *Nano Energy* **2020**, *75*, 104975.
- [17] Feng, Y. W.; Liang, X.; An, J.; Jiang, T.; Wang, Z. L. Soft-contact cylindrical triboelectric-electromagnetic hybrid nanogenerator based on swing structure for ultra-low frequency water wave energy harvesting. *Nano Energy* **2021**, *81*, 105625.
- [18] Liang, X.; Liu, Z. R.; Feng, Y. W.; Han, J. J.; Li, L. L.; An, J.; Chen, P. F.; Jiang, T.; Wang, Z. L. Spherical triboelectric nanogenerator based on spring-assisted swing structure for effective water wave energy harvesting. *Nano Energy* **2021**, *83*, 105836.
- [19] Zhao, L. L.; Duan, J. L.; Liu, L. Q.; Wang, J. W.; Duan, Y. Y.; Vaillant-Roca, L.; Yang, X. Y.; Tang, Q. W. Boosting power conversion efficiency by hybrid triboelectric nanogenerator/silicon tandem solar cell toward rain energy harvesting. *Nano Energy* **2021**, *82*, 105773.
- [20] Liu, X.; Yu, A. F.; Qin, A. M.; Zhai, J. Y. Highly integrated triboelectric nanogenerator for efficiently harvesting raindrop energy. *Adv. Mater. Technol.* **2019**, *4*, 1900608.
- [21] Liang, Q. J.; Yan, X. Q.; Liao, X. Q.; Zhang, Y. Integrated multi-unit transparent triboelectric nanogenerator harvesting rain power for driving electronics. *Nano Energy* **2016**, *25*, 18–25.
- [22] Zhao, Y. Y.; Pang, Z. B.; Duan, J. L.; Duan, Y. Y.; Jiao, Z. B.; Tang, Q. W. Self-powered monoelectrodes made from graphene composite films to harvest rain energy. *Energy* **2018**, *158*, 555–563.
- [23] Nie, S. X.; Guo, H. Y.; Lu, Y. X.; Zhuo, J. T.; Mo, J. L.; Wang, Z. L. Superhydrophobic cellulose paper-based triboelectric nanogenerator for water drop energy harvesting. *Adv. Mater. Technol.* **2020**, *5*, 2000454.
- [24] Peng, X.; Dong, K.; Ning, C.; Cheng, R. W.; Yi, J.; Zhang, Y. H.; Sheng, F. F.; Wu, Z. Y.; Wang, Z. L. All-nanofiber self-powered skin-interfaced real-time respiratory monitoring system for obstructive sleep apnea-hypopnea syndrome diagnosing. *Adv. Funct. Mater.* **2021**, *31*, 2103559.
- [25] Ren, Z. W.; Ding, Y. F.; Nie, J. H.; Wang, F.; Xu, L.; Lin, S. Q.; Chen, X. Y.; Wang, Z. L. Environmental energy harvesting adapting to different weather conditions and self-powered vapor sensor based on humidity-responsive triboelectric nanogenerators. *ACS Appl. Mater. Interfaces* **2019**, *11*, 6143–6153.
- [26] Luo, J. J.; Wang, Z. M.; Xu, L.; Wang, A. C.; Han, K.; Jiang, T.; Lai, Q. S.; Bai, Y.; Tang, W.; Fan, F. R. et al. Flexible and durable wood-based triboelectric nanogenerators for self-powered sensing in athletic big data analytics. *Nat. Commun.* **2019**, *10*, 5147.
- [27] Zhao, J.; Wang, D.; Zhang, F.; Liu, Y.; Chen, B. D.; Wang, Z. L.; Pan, J. S.; Larsson, R.; Shi, Y. J. Real-time and online lubricating oil condition monitoring enabled by triboelectric nanogenerator. *ACS Nano* **2021**, *15*, 11869–11879.
- [28] Wang, Z. M.; An, J.; Nie, J. H.; Luo, J. J.; Shao, J. J.; Jiang, T.; Chen, B. D.; Tang, W.; Wang, Z. L. A self-powered angle sensor at nanoradian-resolution for robotic arms and personalized medicare. *Adv. Mater.* **2020**, *32*, 2001466.
- [29] Zhang, C. G.; Liu, L.; Zhou, L. L.; Yin, X.; Wei, X. L.; Hu, Y. X.; Liu, Y. B.; Chen, S. Y.; Wang, J.; Wang, Z. L. Self-powered sensor for quantifying ocean surface water waves based on triboelectric nanogenerator. *ACS Nano* **2020**, *14*, 7092–7100.
- [30] Pang, Y. K.; Xi, F. B.; Luo, J. J.; Liu, G. X.; Guo, T.; Zhang, C. An alginate film-based degradable triboelectric nanogenerator. *RSC Adv.* **2018**, *8*, 6719–6726.
- [31] Ma, P.; Zhu, H. R.; Lu, H.; Zeng, Y. M.; Zheng, N.; Wang, Z. L.; Cao, X. Design of biodegradable wheat-straw based triboelectric nanogenerator as self-powered sensor for wind detection. *Nano Energy* **2021**, *86*, 106032.
- [32] Ma, J. M.; Zhu, J. Q.; Ma, P.; Jie, Y.; Wang, Z. L.; Cao, X. Fish bladder film-based triboelectric nanogenerator for noncontact position monitoring. *ACS Energy Lett.* **2020**, *5*, 3005–3011.
- [33] Kim, H. J.; Kim, J. H.; Jun, K. W.; Kim, J. H.; Seung, W. C.; Kwon, O. H.; Park, J. Y.; Kim, S. W.; Oh, I. K. Silk nanofiber-networked bio-triboelectric generator: Silk bio-TEG. *Adv. Energy Mater.* **2016**, *6*, 1502329.
- [34] Kim, J. N.; Lee, J.; Go, T. W.; Rajabi-Abhari, A.; Mahato, M.; Park, J. Y.; Lee, H.; Oh, I. K. Skin-attachable and biofriendly chitosan-diatom triboelectric nanogenerator. *Nano Energy* **2020**, *75*, 104904.
- [35] Lu, H.; Zhao, W. Y.; Wang, Z. L.; Cao, X. Sugar-based triboelectric nanogenerators for effectively harvesting vibration energy and sugar quality assessment. *Nano Energy* **2021**, *88*, 106196.
- [36] Xia, K. Q.; Zhu, Z. Y.; Fu, J. M.; Li, Y. M.; Chi, Y.; Zhang, H. Z.; Du, C. L.; Xu, Z. W. A triboelectric nanogenerator based on waste tea leaves and packaging bags for powering electronic office supplies and behavior monitoring. *Nano Energy* **2019**, *60*, 61–71.
- [37] Chen, Y. D.; Jie, Y.; Wang, J.; Ma, J. M.; Jia, X. T.; Dou, W.; Cao, X. Triboelectrification on natural rose petal for harvesting environmental mechanical energy. *Nano Energy* **2018**, *50*, 441–447.
- [38] Wang, N. N.; Zheng, Y. B.; Feng, Y. G.; Zhou, F.; Wang, D. A. Biofilm material based triboelectric nanogenerator with high output performance in 95% humidity environment. *Nano Energy* **2020**, *77*, 105088.
- [39] Liu, D.; Liu, J. M.; Yang, M. S.; Cui, N. Y.; Wang, H. Y.; Gu, L.; Wang, L. F.; Qin, Y. Performance enhanced triboelectric nanogenerator by taking advantage of water in humid environments. *Nano Energy* **2021**, *88*, 106303.